19 October 1998

PHYSICS LETTERS A

ELSEVIER

Physics Letters A 247 (1998) 360–364

Lower threshold field in three-dimensional Josephson-junction arrays

T. Di Matteo [a], J. Paasi [a], A. Tuohimaa [a], R. De Luca [b]

[a] *Laboratory of Electricity and Magnetism, Tampere University of Technology, FIN-33101 Tampere, Finland*
[b] *INFM – Dipartimento di Fisica, Università degli Studi di Salerno, I-84081 Baronissi (Salerno), Italy*

Received 11 May 1998; accepted for publication 28 July 1998
Communicated by J. Flouquet

Abstract

The static magnetic response of a three-dimensional Josephson-junction array is described. The dynamical equations for flux transitions in the network are derived taking into account the magnetic energy of the circulating currents. In particular, when the external magnetic field $\boldsymbol{H}$ is applied in a direction perpendicular to the network-base, we analytically calculate the lower-threshold field $H^{(1)}$. © 1998 Elsevier Science B.V.

PACS: 74.50.+r; 74.25.Ha; 85.25.Dq
Keywords: Josephson effects; Magnetic properties; SQUIDs

1. Introduction

The low-field electromagnetic properties of high-T_c granular superconductors [1] can be well described by means of Josephson junction networks [2,3]. Indeed, these networks can be adopted as equivalent circuital models for this class of superconducting systems [2], which can be thought to be a collection of superconducting grains coupled via Josephson junctions. In this way, an equivalent circuit can be constructed by associating a Josephson junction with each contact region between adjacent grains and an inductor with each current path in order to take account of the self field generated by the current. In particular, it can be shown that there exists a lower threshold field $H^{(1)}$ [4,5] below which a three-dimensional granular superconductor is in the Meissner state. For fields higher than $H^{(1)}$ flux penetration occurs because of 2π phase slips of the junctions located at the system boundaries. Moreover, Josephson junction arrays can be used as model systems of superconducting devices. The extension of these models in three dimensions, therefore, may give rise to a new series of applications. Indeed, these networks can be adopted, as an example, as a first step in realizing magnetic field sensors capable of detecting the local field intensity and direction with very high spatial resolution.

In the present work we therefore study the low-field static magnetic properties of a three-dimensional (3D) array of Josephson junctions [5–7] consisting of n cubes aligned along a fixed direction in space. We derive the dynamical equations for flux transitions in this system in the presence of an externally applied magnetic field $\boldsymbol{H}$. By numerically integrating this set of nonlinear differential equations, the flux and the current distributions are found for $n = 2$. It is shown that the 3D array does present a first threshold field value $H^{(1)}$, below which the system is able to effec-

PII S0375-9601(98)00584-2

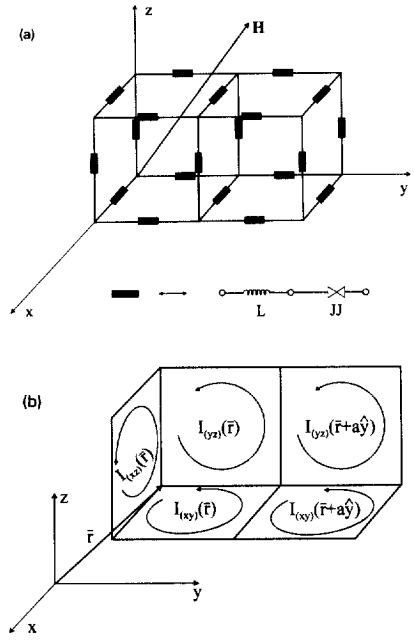

Fig. 1. (a) The circuit model: each box contains an inductor and a Josephson junction, as shown in the inset. (b) Schematic representation of the current variables for two single unit of mutually orthogonal faces in the cubic network.

tively shield the external field. Furthermore, the lower threshold field $H^{(1)}$ in the 3D array with an arbitrary number of cubes can be analytically calculated for external fields applied perpendicular to the network base. These analytic results for $H^{(1)}$ are thus finally compared with the numerical ones computed for $n = 1, 2$.

2. The model dynamical equations

In the present section we write the dynamical equations which govern flux transitions in a 3D network, for different directions of the applied field. The cubic network shown in Fig. 1a, for example, consists of twenty inductively coupled Josephson junctions (JJs) located at the midpoints of the cube sides. Let us then start by associating, with each JJ in the network, a gauge invariant superconducting phase difference $\varphi_\xi(\boldsymbol{r})$, where $\boldsymbol{r} = (x, y, z)$ corresponds to the position of the origin of the unit cell and ξ is the direction along which the junction lies. The flux, Φ, linked to the cube face placed in the cell at position $\boldsymbol{r}$ and lying in the η–ξ plane, can be labelled through a standard tensorial notation. Namely, we take the corresponding normalized flux to be $\Psi_{(\eta\xi)}(\boldsymbol{r}) = \Phi_{(\eta\xi)}(\boldsymbol{r})/\Phi_0$, with Φ_0 being the elementary flux quantum. Moreover, the mesh current I flowing in the η–ξ plane at position $\boldsymbol{r}$ is expressed in terms of a normalized current $i_{(\eta\xi)}(\boldsymbol{r}) = I_{(\eta\xi)}(\boldsymbol{r})/I_{J0}$, where I_{J0} is the maximum Josephson current of the junctions. The currents circulating in a given face are taken to be positive when seen to circulate in the counterclockwise direction by an external observer placed at infinity on the positive side of the axis orthogonal to the face itself (see Fig. 1b).

By imposing fluxoid quantization to each closed loop of the network, one can write the following relations between the Ψ and the φ [5],

$$2\pi\Psi_{(\eta\xi)}(\boldsymbol{r}) = 2\pi n_{(\eta\xi)}(\boldsymbol{r}) + \varphi_\xi(\boldsymbol{r} + a\hat{\boldsymbol{\eta}}) - \varphi_\xi(\boldsymbol{r}) - \varphi_\eta(\boldsymbol{r} + a\hat{\boldsymbol{\xi}}) + \varphi_\eta(\boldsymbol{r}) , \tag{1}$$

where $n_{(\eta\xi)}(\boldsymbol{r})$ are integers and $(\eta\xi)$ takes on the following form: (yz), (zx), (xy). By introducing a translation operator $\hat{T}_\eta$, where the index η gives the direction along which the translation is performed over the distance of a cube side "a", the operator $\hat{T}_\eta$ acts upon the position vector $\boldsymbol{r}$ in the following way [5],

$$\hat{T}_\eta \varphi_\xi(\boldsymbol{r}) = \varphi_\xi(\boldsymbol{r} + a\hat{\boldsymbol{\eta}}) . \tag{2}$$

The same is true for the currents $i_{(\mu\nu)}(\boldsymbol{r})$, the integers $n_{(\mu\nu)}(\boldsymbol{r})$ and the fluxes $\Psi_{(\mu\nu)}(\boldsymbol{r})$. The fluxes and the currents can be expressed in the following compact form,

$$\Psi_{(\eta\xi)}(\boldsymbol{r}) = \sum_{\boldsymbol{r}'}\sum_{\mu\nu} m^{(\mu\nu)}_{(\eta\xi)}(\boldsymbol{r}, \boldsymbol{r}') i_{(\mu\nu)}(\boldsymbol{r}') + \mu_0 \boldsymbol{H}\cdot\boldsymbol{S}_{(\eta\xi)}(\boldsymbol{r}) , \tag{3}$$

where $\boldsymbol{S}_{(\eta\xi)}(\boldsymbol{r})$ is the area vector pertaining to the cube face orthogonal to the η–ξ plane, $m^{(\mu\nu)}_{(\eta\xi)}(\boldsymbol{r}, \boldsymbol{r}')$ are the mutual inductance coefficients between the $(\eta\xi)$ current loop at position $\boldsymbol{r}$ and the $(\mu\nu)$ current loop at position $\boldsymbol{r}'$ and $\boldsymbol{H}$ is the externally applied field.

Moreover, with the aid of the RSJ model [8], for each junction in the network, we can write

$$O_J[\varphi_\xi(\boldsymbol{r})] = \sum_{\mu,\nu} \epsilon_{\xi\mu\nu}[i_{(\xi\nu)}(\boldsymbol{r}) - i_{(\xi\nu)}(\boldsymbol{r} - a\hat{\boldsymbol{\nu}})] , \tag{4}$$

where $\epsilon_{\xi\mu\nu}$ is the Levi-Civita symbol and

$$O_J(\cdot) = \frac{\Phi_0}{2\pi R}\frac{\mathrm{d}}{\mathrm{d}t}(\cdot) + I_J \sin(\cdot) \tag{5}$$

is the nonlinear Josephson operator, with R being the resistive parameter, taken to be the same for all JJs.

The above set of nonlinear ordinary differential equations applies in general to a 3D cubic array of Josephson junctions and must be specialized to the case of a finite system by taking care of setting to zero all the currents which are not present in the system.

3. Static magnetic response

Having derived Eqs. (1)–(5), which completely define the magnetic response of the three-dimensional Josephson junction array, we can now numerically integrate, for $n = 2$, a set of twenty coupled nonlinear differential equations with respect to the phase variables. A standard fourth order Runge–Kutta algorithm is used. The externally applied magnetic field $\boldsymbol{H}$ is taken to lie in the y–z plane and to make an angle θ with respect to the z-axis as in Fig. 1a. By determining the stationary magnetic states after zero-field-cooling (ZFC) we study how the system evolves under a small enough variation $\Delta\boldsymbol{H}$ of the applied field $\boldsymbol{H}$ lying along a fixed direction in space. A similar analysis for $n = 1$ has already been given in a previous work [5].

The flux distribution is obtained by Eq. (1), and the current distribution is derived from Eq. (3) by inverting the mutual inductance matrix $m^{(\mu\nu)}_{(\eta\xi)}(\boldsymbol{r},\boldsymbol{r}')$. Once the values of the model parameters are estimated, the flux and the current distributions can be found. Let us, then, suppose that each face of the cube in Fig. 1a contains a square current loop made of thin cylindrical wires of diameter $2r$. Therefore, for $a = 10$ μm, where a is the length of the cube side, for $a/r = 10^2$ and for maximum Josephson current values of the order of 100 μA, we find $l = 3.3 \times 10^{-11}$ H [9,10], estimating the adimensional SQUID parameter $\beta = lI_{J0}/\Phi_0$ to be of the order of unity. Let us, now, define the mutual inductance values of the m matrix in Eq. (3). Their computation, performed in the same way as in Ref. [5], gives us the following values: $m^{(yz)}_{(xy)}(\boldsymbol{r},\boldsymbol{r})/l = -0.24$; $m^{(yz)}_{(xy)}(\boldsymbol{r},\boldsymbol{r}+a\hat{\boldsymbol{y}})/l = -0.016$; $m^{(yz)}_{(xz)}(\boldsymbol{r},\boldsymbol{r}+2a\hat{\boldsymbol{y}})/l = -0.006$; $m^{(yz)}_{(yz)}(\boldsymbol{r},\boldsymbol{r}+a\hat{\boldsymbol{x}})/l = 0.03$; $m^{(yz)}_{(yz)}(\boldsymbol{r},\boldsymbol{r}+a\hat{\boldsymbol{x}}+a\hat{\boldsymbol{y}})/l = 0.008$; $m^{(yz)}_{(yz)}(\boldsymbol{r},\boldsymbol{r}+a\hat{\boldsymbol{y}})/l = -0.196$ and $m^{(xz)}_{(xz)}(\boldsymbol{r},\boldsymbol{r}+2a\hat{\boldsymbol{y}})/l = 0.006$.

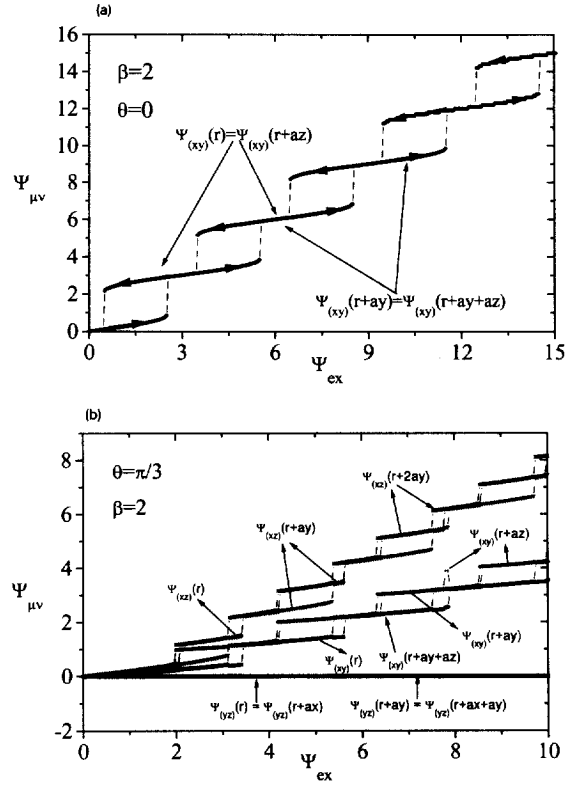

Fig. 2. Flux linked to the eleven cubic faces as a function of the normalized applied flux Ψ_{ex} for $\beta = 2.0$ and for the following field orientations: (a) $\theta = 0$; (b) $\theta = \pi/3$. In (a) we let Ψ_{ex} vary in a cycle in the interval $[0, 15]$. In (b) Ψ_{ex} is taken to increase from 0 to 10.

The resulting flux distributions in the system are shown in Figs. 2a,2b, where $\beta = 2$ has been taken. In Fig. 2a, we plot the normalized flux $\Psi_{(\mu\nu)}$ as a function of the normalized applied flux $\Psi_{ex} = \mu_0 HS_0/\Phi_0$ in the case the externally magnetic field is applied in a direction perpendicular to the base of the network ($\theta = 0$). Let us define a generalized SQUID parameter $\tilde{\beta}_n = L_n I_{J0}/n\Phi_0$ where L_n is an effective inductance associated to the n cubes. Here, as in the case of an r.f. SQUID, we notice that there exists a critical value $\tilde{\beta}^c_n$ below which flux penetration is reversible for any field value. For the chosen value of $\beta = 2$, however, $\tilde{\beta}_2 \geqslant \tilde{\beta}^c_2 = 3/2\pi$ and, at $\Psi_{ex} = \Psi^{(1)}_{ex}$, where $\Psi^{(1)}_{ex}$ is the lower threshold Ψ_{ex}-value, the system shows an irreversible flux transition involving three flux quanta for each cube.

By changing the field direction, a different flux penetration mechanism occurs. This is evident from

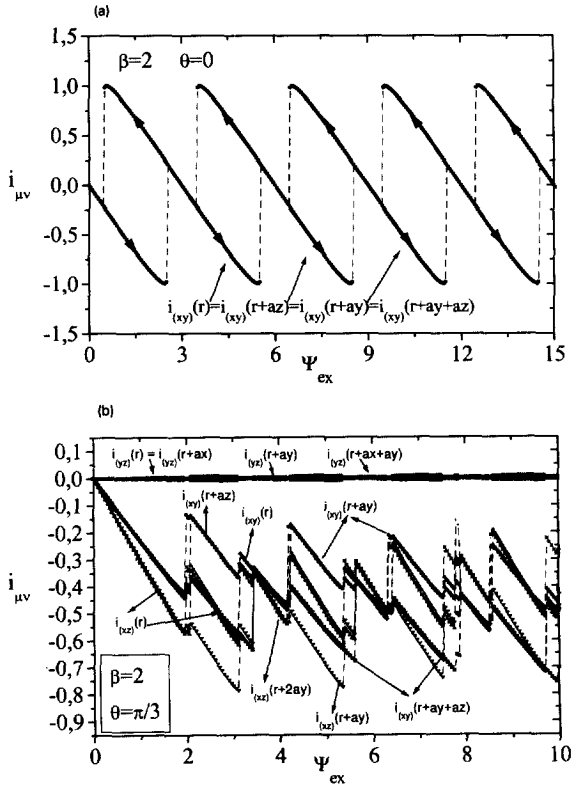

Fig. 3. Mesh currents circulating in the eleven cubic faces as a function of the normalized applied flux Ψ_{ex} for $\beta = 2.0$ and for the following field orientations: (a) $\theta = 0$; (b) $\theta = \pi/3$. In (a) we let Ψ_{ex} vary in a cycle in the interval $[0, 15]$. In (b) Ψ_{ex} is taken to increase from 0 to 10.

Fig. 2b, where $\theta = \pi/3$. In the $\theta \neq 0$ cases we have nonvanishing values of the quantities $\Psi_{(xz)}$. Increasing the θ-value from $\theta = \pi/6$ to $\theta = \pi/2$, for example, it can be seen that the number of fluxons penetrating in the x–z cube faces, at each transition point, increases.

In Figs. 3a,3b, the normalized currents $i_{(\mu\nu)}$ as a function of Ψ_{ex} are reported for $\theta = 0$ and $\theta = \pi/3$, respectively, when $\beta = 2$. These current distributions show discontinuities corresponding to the flux transition values in Figs. 2a,2b.

4. Lower threshold field

Let us, now, analytically derive the lower threshold field for flux penetrations after ZFC in the 3D network consisting of n cubes along the y direction. In what follows we shall take an applied magnetic field $\boldsymbol{H}$ in a direction orthogonal to the n-cubes base, so that an exact analytic solution for $\Psi_{ex}^{(1)}$ can be given. Defining i_b and Ψ_t to be the normalized current circulating in the lower and in the upper base of the network and the normalized flux pertaining to the network, respectively, the current-flux relations can be written as

$$i_{(\mu\nu)} = \Psi_{(\mu\nu)} = 0 \qquad \text{if } (\mu\nu) \neq (xy)\,, \tag{6}$$

$$i_b = \frac{\Psi_t - n\Psi_{ex}}{(L_n I_{J0}/\Phi_0)} \qquad \text{for } (\mu\nu) = (xy)\,, \tag{7}$$

where

$$\begin{aligned} L_n = n[l + m_{(xy)}^{(xy)}(\boldsymbol{r}, \boldsymbol{r} + a\hat{\boldsymbol{z}})] \\ + 2[(n-1)[m_{(xy)}^{(xy)}(\boldsymbol{r}, \boldsymbol{r} + a\hat{\boldsymbol{y}} + a\hat{\boldsymbol{z}}) \\ + m_{(xy)}^{(xy)}(\boldsymbol{r}, \boldsymbol{r} + a\hat{\boldsymbol{y}})] \\ + (n-2)[m_{(xy)}^{(xy)}(\boldsymbol{r}, \boldsymbol{r} + 2a\hat{\boldsymbol{y}} + a\hat{\boldsymbol{z}}) \\ + m_{(xy)}^{(xy)}(\boldsymbol{r}, \boldsymbol{r} + 2a\hat{\boldsymbol{y}})] + \cdots \\ + m_{(xy)}^{(xy)}(\boldsymbol{r}, \boldsymbol{r} + (n-1)a\hat{\boldsymbol{y}} + a\hat{\boldsymbol{z}}) \\ + m_{(xy)}^{(xy)}(\boldsymbol{r}, \boldsymbol{r} + (n-1)a\hat{\boldsymbol{y}})]\,. \end{aligned}$$

For symmetry reasons, the stationary solutions of Eqs. (4) are given by the following,

$$\sin\varphi_x = i_b\,, \tag{8}$$

$$\sin\varphi_y = -i_b\,, \tag{9}$$

$$\sin\varphi_z = 0\,. \tag{10}$$

Moreover, fluxoid quantization gives

$$\Psi_t = -\frac{(n+1)\varphi_b}{\pi}\,, \tag{11}$$

where φ_b is the independent phase variable for all junctions lying in the base face of the network. We may notice that the current flowing in the junctions lying in the shared faces of the cubes is zero. Therefore, the corresponding phase variables are also zero. Substituting Eq. (7) and Eq. (11) in Eqs. (8)–(10), we obtain

$$\Psi_b + \tilde{\beta}_n \sin[n\pi\Psi_b/(n+1)] = \Psi_{ex}\,, \tag{12}$$

where $\Psi_b = \Psi_t/n$. Setting the derivative of Ψ_{ex} with respect to Ψ_b in Eq. (12) equal to zero, the minimum value of $\tilde{\beta}_n$, namely $\tilde{\beta}_n^c = (n+1)/n\pi$, can be found.

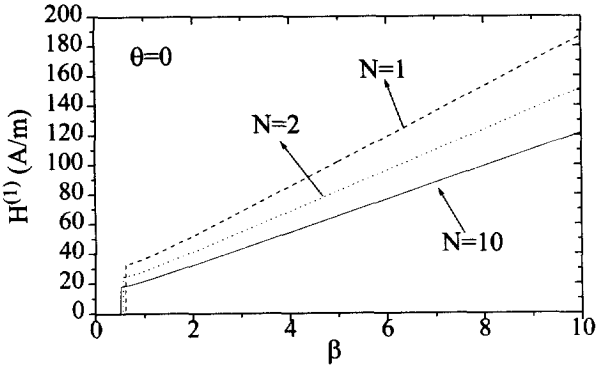

Fig. 4. Lower threshold field in a 3D network as a function of the SQUID parameter β for an axially applied external magnetic field for $n = 1, 2$ and 10.

The lower threshold flux value,

$$\Psi_{ex}^{(1)} = \tilde{\beta}_n \sqrt{1 - \left(\frac{n+1}{n\pi\tilde{\beta}_n}\right)^2} + \frac{n+1}{n\pi}\left[\pi - \sin^{-1}\sqrt{1 - \left(\frac{n+1}{n\pi\tilde{\beta}_n}\right)^2}\right], \qquad (13)$$

can be derived by solving simultaneously Eq. (12) and the equation obtained by setting $d\Psi_{ex}/d\Psi_b = 0$.

Let us, now, introduce the lower threshold field, $H^{(1)}$, which is proportional to $\Psi_{ex}^{(1)}$ through the constant factor $\Phi_0/\mu_0 S_0$. In Fig. 4, we compare the analytical $H^{(1)}$ behaviour in terms of β for $n = 1$, 2 and 10 when $\theta = 0$. In this figure the $\tilde{\beta}_n$ values are $\tilde{\beta}_1 = 1.03\beta$, $\tilde{\beta}_2 = 0.84\beta$ and $\tilde{\beta}_{10} = 0.68\beta$ for the 3D-network consisting of one cube, two and ten cubes along the y-direction, respectively. These parameters are computed by substituting the $m_{(\eta\xi)}^{(\mu\nu)}(\boldsymbol{r}, \boldsymbol{r}')$ coefficients into the expression for L_n and then by setting $\tilde{\beta}_n = (1/n)(L_n/l)\beta$. We may notice that increasing the number of cubes in the network, the $H^{(1)}$ and $\tilde{\beta}_n^c$ values decrease. Finally, a numerical evaluation of $H^{(1)}$ is shown in Fig. 5, for $n = 1, 2$ and $\theta = 0$. This evaluation for $H^{(1)}$ is done by inspection on the numerical $\Psi_{(\mu\nu)}$ vs $\Psi_{(ex)}$ curves. Indeed, by taking the value of $\Psi_{(ex)}$ corresponding to the first irreversible flux transition in the system and by defining this value as $\Psi_{ex}^{(1)}$, one can set $H^{(1)} = (\Phi_0/\mu_0 S_0)\Psi_{ex}^{(1)}$. As it can be seen from Fig. 5, the numerical and analytical evaluations of $H^{(1)}$ are in agreement.

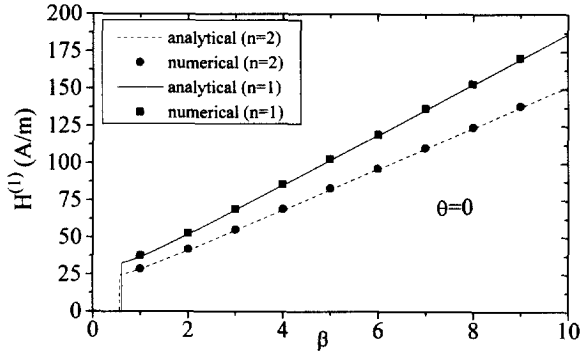

Fig. 5. Lower threshold field in a 3D network as a function of the SQUID parameter β for an axially applied external magnetic field for $n = 1$ and 2.

5. Conclusions

We have studied the low-field static magnetic properties of a three-dimensional array of Josephson junctions. In this framework, the dynamical equations for flux transitions have been derived for n-cubes lying in a fixed direction in space. We have numerically calculated the expression for the lower threshold field $H^{(1)}$ for $n = 2$ and for an external magnetic field orthogonal to the base of the array. A general analytic solution for $H^{(1)}$ is also derived for an arbitrary number of cubes for $\theta = 0$.

Acknowledgement

We thank Professor S. Pace for many helpful discussions and CIMO for financial support.

References

[1] J.G. Bednorz, K.A. Müller, Z. Phys. B 64 (1986) 189.
[2] J.R. Clem, Physica C 153–155 (1988) 50.
[3] M. Tinkham, C.J. Lobb, Solid State Phys. 42 (1989) 91.
[4] M.A. Zelikman, Supercond. Sci. Technol. 7 (1997) 469.
[5] R. De Luca, T. Di Matteo, A. Tuohimaa, J. Paasi, Phys. Rev. B 57 (1998) 1173.
[6] R. De Luca, S. Pace, C. Auletta, G. Raiconi, Phys. Rev. B 52 (1995) 7474.
[7] S.P. Yukon, N. Chu, H. Lin, IEEE Trans. Applied Supercond. 5 (1995) 2959.
[8] A. Barone, G. Paternó, Physics and Applications of the Josephson Effect (Wiley, New York, 1982).
[9] D. Reinel, W. Dieterich, T. Wolf, A. Majhofer, Phys. Rev. B 49 (1994) 9118.
[10] E. Weber, Electromagnetic Fields (Wiley, New York, 1954).